

Accepted version on Author's Personal Website: Armin Norouzi

Citation:

Norouzi, Armin, Reza Kazemi, and Omid Reza Abbassi. "Path planning and re-planning of lane change manoeuvres in dynamic traffic environments." *International Journal of Vehicle Autonomous Systems* 14.3 (2019): 239-264.

See also:

https://arminnorouzi.github.io/files/pdf/path_planning_accepted_version-wfp.pdf

As per publisher copyright is ©2019



This work is licensed under a [Creative Commons Attribution-NonCommercial-NoDerivatives 4.0 International License](https://creativecommons.org/licenses/by-nc-nd/4.0/).



Article accepted version starts on the next page →
[Or link: to Author's Website](#)

Path planning and re-planning of lane change maneuvers in dynamic traffic environments

Armin Norouzi^{*1}, Reza Kazemi², Omid Reza Abbasi³

¹ Department of Mechanical engineering, Faculty of Engineering, University of Alberta, Edmonton, AB, Canada. Email: norouziy@ualberta.ca

² Faculty of Mechanical Engineering, K.N. Toosi University of Technology, Tehran, Iran. Email: kazemi@kntu.ac.ir

³ Faculty of Geodesy and Geomatics Engineering, K.N. Toosi University of Technology, Tehran, Iran. Email: oabbasi@mail.kntu.ac.ir

* Correspond Author, Address: Department of Mechanical Engineering, Faculty of Engineering, University of Alberta, AB, Canada. Email: norouziy@ualberta.ca, Tel: +1 587 987 1300

Abstract

Automatic lane change is of utmost importance in designing autonomous vehicles and Driver Assistant Systems. In this study, a novel path for lane change maneuvers, based on mathematical functions, is introduced. To obtain a suitable path for lane change maneuvers, four functions, namely quintic, septic, sinusoidal, and tangent functions, were examined. The analysis revealed that, according to the ISO Standards and peak acceleration criterion, a quintic function has the advantage of passenger comfort over other path functions. After choosing the appropriate path, an algorithm for re-planning the lane change path, based on dynamic traffic conditions, was proposed. The simulation results show that the proposed algorithm is capable of designing the path in various traffic conditions. Moreover, the algorithm can navigate the vehicle to the initial lane, if the maneuver is not possible. Our analytical results showed that the designed paths are suitable, comfortable, and safe.

Keywords

Automatic lane change; autonomous vehicle; path planning; lane change re-planning

1. Introduction

Yearly, a high number of losses occur in road accidents. Drowsiness and driver fatigue are among the most important causes of fatal accidents. In recent years, vehicle engineers have presented some intelligent driver assistant systems to improve the autonomous vehicles. Advanced Driver Assistance Systems (ADAS) enhance the safety and better driving. Lane Keeping System (LKS), Driver Drowsiness Detect, Lane Departure Warning (LDW), and Lane Changing Assistance are examples of ADAS (1). One of the significant works emerging today is the development of a system which can control the vehicle in emergency situations. Such a system should detect the drowsiness and driver fatigue, guarantee the safety and stability of maneuver, generate an appropriate path with the traffic of road taken into account, and track the generated path. This system is shown in Figure 1.

[Insert Figure 1]

When the system detects the drowsiness of the driver, the decision-making system evaluates the conditions of maneuver and the automatic lane change system navigates the vehicle to the roadside. The main components of an automatic lane change system are also shown in Figure 1.

The automatic lane change systems operate as follows: The decision making system determines the required time for lane changing maneuver. Then, the path planning system generates the appropriate path. Thus, a change in the required time would result in changes in the path. The final component provides the ability to track the generated path.

The lane change maneuver, in addition to emergency situations, is of particular importance in autonomous vehicles. For example, the takeover maneuver includes two (double) lane changes. So, generating a path in which the lane can be changed safely and smoothly is an applicable topic in autonomous vehicle problems. Various studies have focused on this problem using different approaches, models, and assumptions.

Some researchers (2, 3) have used polar and Cartesian versions of quintic polynomial functions to generate the appropriate path. Chee et al. (4) used circular and cosine functions, quintic polynomials, and Trapezoidal acceleration trajectories, and resulted that the latter is better in terms of ride comfort. Moreover, Chen et al. (5) have considered a Bezier curve as the path. These works have studied the statics of the problem and do not consider the dynamical aspects of the traffic.

The Hidden Markov Model (HMM) has been extensively used in some studies (6-8). The main disadvantage in these methods is that experimental data are required to train the model. Choi et al. (9) have used Geospatial Information Systems (GIS) to determine whether the autonomous vehicles change the lane or not when detecting an obstacle. Furthermore, Li et al.(10) and Chu et al.(11) have used a vehicle dynamic constrained model in which the path is generated more accurately, however, there is no option for re-planning the path.

Some papers (12) have utilized a potential field method to model the path planning. The approach has the ability to consider the curvature of the path. For instance, Sattel and Brandt (13) have proposed a potential field path-planning algorithm for shared lateral guidance with the driver considered in the path planning and vehicle navigation. The main disadvantage of these methods is that it is difficult to implement vehicle kinematics and ambient dynamics.

Li et al. (14) have employed polynomial functions and have provided some abilities in which more control could be brought to the vehicle. These include lane keeping, lane changing, vehicle tracking, and avoiding collision with static and moving objects. However, the authors have not considered the uncertainty issues resulting from localization, not perception.

Lan and DiCairano (15) have applied a Rapidly-Exploring Random Tree Star (RRT)-based algorithm to deal with sudden changes in the environment. The algorithm employs a re-planning procedure to rapidly react to changes in a real-time manner. However, the uncertainties in obstacle position and vehicle dynamics were not included in the research.

Wang et al. (16) have employed a linear offset and sinusoidal function to guarantee the passenger's safety and comfort in maneuvers, and to provide a path which has a low-curvature in lane changing. Some other researchers (17) have addressed the problem of lane changing in curved parts of the roads using sine/cosine functions based on vehicle dynamics constraints. However, the presence of other vehicles in the road and path re-planning using road dynamics have not addressed in these papers.

Perumal et al. (18) have conducted a research based on Kalman Filter to predict the vehicle and obstacle positions. But it lacks the aspects of driver safety, and the generated paths are not necessarily optimum.

In a research conducted by Zips et al. (19), a fast optimization process has been developed based on static obstacles. However, this algorithm is not capable of regenerating the path with respect to movements of obstacles. Moreover, the driver safety has not been addressed in this research.

Sun et al. (20) have conducted a research regarding the prediction of movements of other vehicles by applying dynamic constraints. The inclusion of movements of other vehicles is advantageous, but the omission of the longitudinal dynamics of the vehicle and applying severe constraints on path design have reduced the applicability of the proposed method.

A review on the research background reveals that some issues in the path planning of autonomous vehicle have not still been resolved. The re-planning problem when the vehicle cannot remain in the designed path, and comparing different polynomial functions have not been highlighted in previous researches. Addressing these problems is the main goal of the present research. Therefore, the paper's contribution can be summarized as follows:

- 1- Analyzing different polynomial functions to find the best function based on both lateral RMS and maximum acceleration, and based on ISO 2631-1 Standard.
- 2- Proposing a comprehensive method for re-planning based on road traffic.
- 3- Proposing a return algorithm during the maneuver.
- 4- Evaluating the proposed algorithms and illustrating their working limits.

In what follows, the concept of the proposed algorithm and mathematical equations are discussed in Sections 2 and 3, respectively. The simulation results are presented in Section 4. Finally, Section 5 concludes the paper.

2. Concept

As shown in Figure 1, the components of the automatic lane change system include the decision-making system, the path planning system, and the tracking control system. The decision-making system, based on sensors, radars, images, and videos, among others, determines the required time for starting (t) and ending (T) the maneuver. Then, the path planning system generates a path with respect to t and T . If, in the process of changing the lane, t or T changes, a new path will be generated. Each vehicle in a road has its own position, velocity, and acceleration. Hence, due to the existing uncertainties in the road and traffic conditions, path re-planning is essential. Figure 2 depicts a vehicle that its path should be changed. Supposing constant velocities for vehicles A and B, and a safe distance between vehicles, t_1 and T_1 can be obtained from the decision-making system. Path re-planning occurs when, after the generation of the path, A or B accelerates. Thus, a new set of time variables (t_2 and T_2) is introduced to the path generation system. If either vehicle A increases its velocity or vehicle B reduces its velocity, the distance between vehicles becomes unsafe. In each situation, according to Figure 3(a) and 3(b), a new path will be generated. If both situations happen, the decision-making system detects that the maneuver is unsafe and the re-planning path will be generated. In this study, based on this procedure, the re-planning is applied.

[Insert Figure 2]

[Insert Figure 3]

3. Methodology

This paper includes two parts: Choosing an appropriate path function based on several criteria and re-planning the path using the selected path function. It is assumed that the safe maneuver's duration has been obtained from the decision-making system, taken the environment sensors data into account, which guarantees the vehicle stability. It is also assumed that the re-planning duration (initial time and proper final time) has been obtained from the decision-making system. Moreover, the longitudinal velocity is assumed to be constant during the maneuver.

Since, in the beginning and at the end of the maneuver, denoted by t_1 and T_1 , only the longitudinal dynamics exist, the lateral velocity and acceleration are zero. So, the boundary conditions are as follows:

$$\dot{y}|_{t=t_1} = 0 \quad (1)$$

$$\ddot{y}|_{t=t_1} = 0 \quad (2)$$

$$\dot{y}|_{t=T_1} = 0 \quad (3)$$

$$\ddot{y}|_{t=T_1} = 0 \quad (4)$$

The origin of the coordinate system is considered at t_1 . So:

$$y|_{t=t_1} = 0 \quad (5)$$

Another condition is that the path function should coincide with centerline at the end of the maneuver. Thus, the cost function is formed as follows:

$$\text{cost function} = (y_1|_{t=T_1} + 3.75)^2 \quad (6)$$

If we have six unknowns, the above system of equations would become a deterministic system. Thus, optimization becomes meaningless. Then, Equation (6) would become:

$$y_1|_{t=T_1} = -3.75 \quad (7)$$

The road lane width is 3.75 meters, based on Interstate Highway Standards for the U.S. Interstate Highway System. In other words, the distance between the centerline of the first lane and the second lane is 2.75 meters.

In the re-planning mode, the boundary conditions in the beginning ($t = t_2$) include the continuity of the path function and its first and second derivatives.

$$(y_2 = y_1)|_{t=t_2} \quad (8)$$

$$(\dot{y}_2 = \dot{y}_1)|_{t=t_2} \quad (9)$$

$$(\ddot{y}_2 = \ddot{y}_1)|_{t=t_2} \quad (10)$$

The boundary conditions at the end of the newly generated path is similar to Equations (3), (4), (6) and (7). Based on the visual analysis of the behavior of the functions and previous works, we considered the following functions to generate the path.

$$y_{c,1}(t) = at^5 + bt^4 + ct^3 + dt^2 + et + f \quad (11)$$

$$y_{c,2}(t) = at^7 + bt^6 + ct^5 + dt^4 + et^3 + ft^2 + gt + h \quad (12)$$

$$y_{c,3}(t) = \sin(bt + c) + dt^3 + et^2 + ft + g \quad (13)$$

$$y_{c,4}(t) = \tan^{-1}(bt) + ct^3 + dt^2 + et + f \quad (14)$$

where $y(t)$ is the lateral position of the vehicle in meters and t is the time. Substituting the boundary conditions in Equations (11) and (14) yields six equations and six unknown parameters. Thus, optimization is not required and Equation (7) is used. The boundary conditions in (1) through (5) were also applied to Equations (12) and (13). **By doing this, all the obtained parameters are based on parameter sets (a,b) and (a, b, c) for $y_{c,3}$ and $y_{c,4}$, respectively. Therefore, the cost functions are defined as Equations (15) and (16) in order to be able to obtain these unknown parameters.** In this study, we used Artificial Bee Colony (ABC) optimization algorithm to determine the optimum parameters. The performance of this algorithm is better **than** or similar to that of other algorithms. Nevertheless, the algorithm uses fewer control parameters (21).

$$\text{cost function} = (\sin(bT_1 + c(a, b)) + d(a, b)T_1^3 + e(a, b)T_1^2 + f(a, b)T_1 + g(a, b) + 3.75)^2 \quad (15)$$

$$\text{cost function} = (aT_1^7 + bT_1^6 + cT_1^5 + d(a, b, c)T_1^4 + e(a, b, c)T_1^3 + 3.75)^2 \quad (16)$$

In this study, based on the traffic conditions, the following modes have been considered:

(1) Path design and choosing the appropriate path function. In this step, t_l and T_l are introduced as inputs obtained from the decision-making system. Note that the initial path starts at $t_l=0$. The objective of this step is to compare different paths and find the best one. This step is shown schematically in Figure 2.

(2) Re-planning: Since the vehicle has not entered a new lane, the maneuver is possible. In t_i , according to the traffic conditions, the decision-making system determines a new T_i . Because $y(t_i) < H/2$, where H is the line width, the path planning system generates a new path for completing the maneuver. This mode is shown in Figures 3(a) and 3(b).

(3) Return re-planning: The vehicle has entered the new lane and the decision-making system has reported the unsafe maneuver. In this mode, because $y(t_i) > H/2$, the vehicle should be returned to the previous lane. This mode is shown in Figure 3(c).

Based on the proposed scenario, our problem-solving algorithm is shown in Figure 4. When $i=I$, this algorithm examines Equations (11) through (14), and when $i>I$, the algorithm enters the re-planning mode.

The pseudo-code of the Artificial Bee Colony optimization algorithm is shown in Figure 5.

[Insert Figure 4]

[Insert Figure 5]

4. Simulation results and discussion

4.1. Suitable path selection

In this paper, we present an algorithm to select an appropriate path in terms of passenger comfort.

For selecting the path, we used ISO 2631-1 Standard (22). This standard relates comfort with the overall RMS acceleration acting on the human body.

The overall RMS acceleration acting on the human body is defined as:

$$a_{\omega} = \sqrt{k_x^2 \cdot a_{\omega x}^2 + k_y^2 \cdot a_{\omega y}^2 + k_z^2 \cdot a_{\omega z}^2} \quad (17)$$

where a_{wx} , a_{wy} , and a_{wz} are longitudinal, lateral, and ride accelerations, respectively. In our study, the longitudinal and ride accelerations are zero. Moreover, k_x , k_y , and k_z are multiplying factors. Thus, the overall RMS acceleration in our problem ($k_y=1.4$ (23)) is:

$$a_{\omega} = 1.4 \times a_{\omega y} \quad (18)$$

The thresholds for overall acceleration, according to the standard, and their corresponding lateral accelerations are shown in Table 1.

Table 1. Overall and lateral RMS ranges according to ISO 2631-1 Standard (22)

Consequence	Overall Acceleration	Lateral Acceleration
Not uncomfortable	$a_{\omega} < 0.315 \text{ m/s}^2$	$a_{y\omega} < 0.225 \text{ m/s}^2$
A little uncomfortable	$0.315 < a_{\omega} < 0.63 \text{ m/s}^2$	$0.225 < a_{y\omega} < 0.45 \text{ m/s}^2$
Fairly uncomfortable	$0.5 < a_{\omega} < 1 \text{ m/s}^2$	$0.357 < a_{y\omega} < 0.714 \text{ m/s}^2$
Uncomfortable	$0.8 < a_{\omega} < 1.6 \text{ m/s}^2$	$0.571 < a_{y\omega} < 1.143 \text{ m/s}^2$
Very uncomfortable	$1.25 < a_{\omega} < 2.5 \text{ m/s}^2$	$0.893 < a_{y\omega} < 1.786 \text{ m/s}^2$
Extremely uncomfortable	$a_{\omega} > 2.5 \text{ m/s}^2$	$a_{y\omega} > 1.786 \text{ m/s}^2$

The other measure used in this study is the peak acceleration. The path with lowest peak acceleration is the appropriate path. In order to examine the above measures, we define a K_a factor as:

$$k_a = a_{\text{RMSy}} \times a_{\text{peak}} \quad (19)$$

where a_{RMSy} is the lateral RMS acceleration, and a_{peak} is the maximum value of lateral acceleration.

Using this measure, we can evaluate our functions and, finally, select the appropriate path for lane changing. The paths for $y_{c,3}$ and $y_{c,4}$ are different, because the optimization algorithm proposed different values for parameters. Figures 6 and 7 illustrate the paths generated using quintic and sinusoidal functions and the corresponding lateral accelerations. Due to the fluctuations in the plot and the roughness of the generated paths, Paths 4 to 6 were eliminated. Noting the similarities

between Paths 1, 2, and 3, we selected path 3 to compare it with the others. The lane changing path based on septic function is shown in Figure 8. Because of the similarities among paths, the one which is finally closer to the target lane (Path 4) is selected to be compared to the others.

[insert Figure 6]

[insert Figure 7]

[insert Figure 8]

Figures 9 (a) and (b) show the tangent paths and their corresponding accelerations, respectively. As shown, Paths 1, 3, and 4 are not good enough, as their peak acceleration is high. From these paths, we selected Paths 2 and 5 to compare with other paths.

[Insert Figure 9]

Finally, Figure 10(a) illustrates the selected paths in the same plot. The figure depicts Path 3 from sinusoidal paths, the quintic path, Path 4 from septic paths, and Paths 2 and 5 from tangent paths. Also, Figure 10(a) illustrates corresponding accelerations. Visually, the sinusoidal, quintic, and septic paths are more suitable for lane changing.

[Insert Figure 10]

As Figure 10(b) suggests, the tangent path (5) is not appropriate for lane changing. So, we abandoned it. The four remaining paths will be compared based on standards and measures. Figure 11 indicates three different measures for the four remaining paths.

[Insert Figure 11]

Figure 11 suggests that the tangent path has better performance over the others in terms of lateral acceleration, but its peak acceleration is so high. The other functions performances are similar, but the quintic path performance is, to some extent, better. We also integrated the two measures using a K_a factor to be able to compare the results more accurately. Again, the quintic function had the lowest value. Practically, it seems that the sinusoidal and septic functions are not appropriate, due to their long solving time. It can be resulted that the quintic function is an appropriate path according to ISO 2631-1 standards, peak acceleration, and K_a factor. The quintic path, according to the noted standard, is “a little uncomfortable”. Noting the emergency situation of lane changing, it can be a good result.

4.2.Re-planning example and simulation

We present three practical examples of the re-planning problem. In the following examples, completing the maneuver has a high risk. Therefore, re-planning is essential to guarantee the safety of maneuver. CarSim software was used to simulate the examples (24). The velocity of the vehicle in the simulation was 108 km/h.

Case 1: Reported by the decision-making system, the lane change starts at 0 second and ends in 6 seconds. Thus, after 0.9 seconds from the start of maneuver, the ending time of the maneuver would change to 7 seconds. These changes would result in a new path constrained by the new starting and ending times. Also, after 2.4 seconds from the starting point of the maneuver, the

ending time would change to 5 seconds, and the new path would start at 4.2 seconds. In this example, the ending time of the maneuver has changed for three times, so the re-planning system should correspondingly design three new paths. Starting and ending times of the maneuver are shown in Table 2. The term y_i is the path number in each re-planning, y_1 is the maneuver's lateral position from t_1 to T_1 , y_2 is the maneuver's lateral position from t_2 to T_2 , and y_3 is the maneuver's lateral position from t_3 to T_3 .

Table 2. Re-planning time (Example 1)

	t_i [s]	T_i [s]
$y_1(t)$	0	6
$y_2(t)$	0.9	7
$y_3(t)$	2.4	5

Regarding the data and the numeric value for $Y(t_i)$ which is lower than the half of the lane change path, the vehicle need not be returned to its previous lane. Hence, the maneuver is feasible. Figure 12(a) shows the designed functions. Functions 2 and 3 have been re-planned based on the dynamics of the road. The final path of lane changing is shown in Figure 12(b).

Figure 13 illustrates the simulation of Example 1. As is apparent in Figure 13(a), the controller system of CarSim has a good performance, and perfectly follows the desired path. Figure 13(b) shows the steering angle and Figures 13(c) and 13(d) show the lateral acceleration and yaw rate, respectively.

[Insert Figure 12]

[Insert Figure 13]

The overall acceleration of maneuver in this example is 1.7579 m/s^2 . This acceleration, based on the standard, is "very uncomfortable". The RMS accelerations for the other paths are 0.3777, 0.4119, and 0.9683, respectively for paths 1, 2, and 3. Therefore, it can be resulted that when the ending time of the maneuver approaches to the required time for re-planning, the designed paths would have high RMS acceleration.

Case 2: In this case, the starting time of the lane change is at 0 second and the ending time of the maneuver is at 6 seconds. Thus, 1.2 seconds after the start of the maneuver, the ending time of the maneuver would change to 4.5 seconds. Again, these changes would result in a new path constrained by the new starting and ending times. In addition, 2.1 seconds after the starting point of maneuver, the ending time would change to 5 seconds, and the new path would start at 5.5 seconds. In this example, the ending time of the maneuver has also changed for three times, so the re-planning system should design three new paths. Starting and ending times of the maneuver are shown in Table 3.

Table 3. Re-planning time (Example 2)

	t_i [s]	T_i [s]
$y_1(t)$	0	6
$y_2(t)$	1.2	4.5
$y_3(t)$	2.1	5.5

Similar to the previous case, the vehicle need not be returned to the initial lane and the maneuver is feasible. Figure 14(a) illustrates the three designed paths. Also, Figure 14(b) shows the final path of lane changing.

[Insert Figure 14]

Figure 15 illustrates the simulation of Example 2. As is apparent in Figure 15(a), the controller system of CarSim has a good performance, and perfectly follows the desired path. Figure 15(b) shows the steering angle, and Figures 15(c) and 15(d) show the lateral acceleration and yaw rate, respectively.

[Insert Figure 15]

The overall RMS acceleration of the lane changing path is 4.6758. The RMS accelerations for path functions 1, 2, and 3 are, respectively, 0.4361, 1.0782, and 3.1615. It can be seen that, as t_i approaches the T_i , the maneuver time would become shorter. The shorter the maneuver, the higher the RMS, particularly in the case of the re-planned path 3.

Case 3: In this example, taking the positions of other vehicles with respect to the target vehicle into account, the decision-making system orders three re-planning designs. Initially, the maneuver starts at 0 and ends in 6 seconds. After 1.2 and 1.9 seconds from the starting point, the ending point would change to 5 and 7 seconds, respectively. Since, in this case, the vehicle has passed the centerline and an accident is highly possible, the decision-making system should return the vehicle to the initial lane. The required return time, reported by the decision-making system, is 6.5 seconds. Again, in this example, the ending time of the maneuver has also changed for three times, so the re-planning system should design three corresponding new paths. The difference of this example with the previous examples is that the third path is toward the initial lane and the maneuver is not accomplished. Starting and ending times of maneuver are shown in Table 4.

Table 4. Re-planning time (Example 3)

	t_i [s]	T_i [s]
$y_1(t)$	0	6
$y_2(t)$	1.2	5
$y_3(t)$	1.9	7
$y_4(t)$	3.1	6.5

Figure 16(a) illustrates the re-planning of the path and the returning process to the initial lane. Figure 16(b) shows the final path. The goal of the path design is to avoid an accident.

[Insert Figure 16]

Figure 17 illustrates the simulation of Example 3. As is apparent in Figure 17(a), the controller system of CarSim has a good performance, and perfectly follows the desired path. Figure 17(b)

shows the steering angle, and Figures 17(c) and 17(d) show the lateral acceleration and yaw rate, respectively.

[Insert Figure 17]

The overall RMS acceleration for this maneuver is 3.2113. Moreover, RMS values for functions 1 through 4 are, respectively, 0.4361, 0.8140, 0.4086, and 1.5526. As seen, the vehicle sustains high acceleration when its path changes from 3 to 4. Generally, the designed paths are not suitable in terms of passenger comfort, but considering the avoidance from an accident, the system is very accurate. In fact, the vehicle should change its path about 60 to 90 degrees in only a few seconds. This abrupt change in the path would result in high values of acceleration.

In order to examine the performance of the proposed algorithm, we analyze the values of RMS with respect to re-planning maneuver time periods by using mathematical equations which are proposed in Methodology section. For this, we introduce two variables a and b :

$$a = t_2 - t_1 \quad (20)$$

$$b = \frac{T_2}{T_1} \quad (21)$$

Figures 18 (a) and (b) illustrate the variations of RMS with respect to b for different values of a . In these plots, T_1 is 10 seconds. As b is in the range of 0.4 to 1, T_2 is between 4 and 10. In other words, this analysis is for re-planned paths in which the ending time of the maneuver is lower than the previous ending time.

[Insert Figure 18]

These plots, in general, have similar behaviors. What is common between the plots is that for low values of a , the value of b has no influence on RMS. But, as a increases, b also increases to reach a suitable acceleration. This increment is directly related to the value of a . For the case in which the vehicle completes the maneuver, when a is lower than 1.2, the acceleration has no significant variations with different values of b . a is the maximum time between two consecutive orders for changing the path. If this parameter is greater than 1.2, some values of b will result in high accelerations. For example, if the value of a and b are 2.4 and 0.4, respectively, the RMS value is greater than 4. In this case, for values of b that are greater than 0.6, the results are more suitable. Thus, when T_1 is 10 seconds, T_2 becomes equal to 6 seconds. In other words, for maneuver durations greater than 6 seconds, the maneuver is more comfortable. It should be noted that the order time for lane changing is also important. As the value of a increases (delay in the order time), suitable values of b become greater. For the case in which the vehicle should be returned to the initial lane, as a increases and the value of b is low, the acceleration increases. For each a , there is a value for b from that on the acceleration value has no variations. For example, when values of a and b are 2.4 and 0.4 respectively, the RMS value is more than 1. In this case, the results are more suitable when the values of b are more than 0.6. Again, delays in ordering the re-planning mode might result in higher risks. Based on the results obtained from the plots, more negligible

differences between T_1 and T_2 ($T_1 > T_2$) would result in more acceptable performance. Moreover, when the values of t_1 and t_2 are close to each other, the proposed algorithm presents more desirable results.

Variations of T_1 with respect to the RMS acceleration are shown in Figure 19. When a is constant, increasing T_1 will result in less variations in RMS acceleration. Note that Figure 19 depicts the case in which the maneuver of lane changing is feasible. In addition, as a increases, these variations also will be amplified. For instance, when a is 1.2 and T_1 is 8 seconds (the black curve), for values of b greater than 0.8, the RMS acceleration is acceptable, according to the standard. In this case, the value of T_2 would be 6.4. This example reveals that in the previous examples critical situations have been considered.

[Insert Figure 19]

Figure 20 depicts the situation in which T_2 is greater than T_1 . As seen, for smaller values of T_1 , there are higher variations in the RMS value. This can be attributed to the short maneuver time. However, for greater values of T_1 , these variations are insignificant. For instance, when T_1 is 3 seconds, the entire path should be passed in 3 seconds. This will be resulted in high RMS acceleration. But, when T_1 is equal to 6 seconds, RMS value is acceptable. Therefore, it can be resulted that the proposed algorithm shows better performance when $T_1 < T_2$, according to the ISO 2631-1 standards.

[insert Figure 20]

5. Conclusions

In this paper, we studied the lane changing path design in automatic lane changing systems. To obtain suitable path function for lane changing, four different functions including quintic, septic, sinusoidal, and tangent functions were examined. According to the ISO 2631-1 standards and the peak RMS acceleration, a quintic path is more comfortable in lane changing. So, based on this path, an algorithm for path re-planning using the decision-making system was proposed. The re-planning problem was examined in three different examples. Moreover, the impact of the starting and ending time of initial path, and the starting and ending time of the re-planned path on the RMS acceleration value was examined. Then, the simulations were conducted using carSim. The simulation results show that the proposed algorithm is capable of designing the path in many traffic conditions. Our analytical results showed that when $T_1 > T_2$ and their difference is small, the proposed algorithm has better performance. In addition, when the difference between t_1 and t_2 is small, the proposed algorithm has better performance. Moreover, it can be concluded that when $T_2 > T_1$, as T_1 increases, the proportion T_2/T_1 has lower impact on the RMS value. Finally, the proposed algorithm has better performance for $T_2 < T_1$, than $T_2 > T_1$. Future works can alter the algorithm to a real-time one to be applied in real-world situations. Additionally, one can consider the impact of the longitudinal velocity on the re-planning system.

Conflict of interests

The authors declare no conflict of interests.

References

1. Fatigue D. Road Accidents: A Literature Review and Position Paper. The Royal Society for the Prevention of Accidents. 2001.
2. Nelson W, editor Continuous-curvature paths for autonomous vehicles. Robotics and Automation, 1989 Proceedings, 1989 IEEE International Conference on; 1989: IEEE.
3. Norouzi A, Kazemi R, Azadi S. Vehicle lateral control in the presence of uncertainty for lane change maneuver using adaptive sliding mode control with fuzzy boundary layer. Proceedings of the Institution of Mechanical Engineers, Part I: Journal of Systems and Control Engineering. 2018;232(1):12-28.
4. Chee W, Tomizuka M. Vehicle lane change maneuver in automated highway systems. California Partners for Advanced Transit and Highways (PATH). 1994.
5. Chen J, Zhao P, Mei T, Liang H, editors. Lane change path planning based on piecewise Bezier curve for autonomous vehicle. Vehicular Electronics and Safety (ICVES), 2013 IEEE International Conference on; 2013: IEEE.
6. Nishiwaki Y, Miyajima C, Kitaoka N, Terashima R, Wakita T, Takeda K, editors. Generating lane-change trajectories of individual drivers. Vehicular Electronics and Safety, 2008 ICVES 2008 IEEE International Conference on; 2008: IEEE.
7. You F, Zhang R, Lie G, Wang H, Wen H, Xu J. Trajectory planning and tracking control for autonomous lane change maneuver based on the cooperative vehicle infrastructure system. Expert Systems with Applications. 2015;42(14):5932-46.
8. Oliver N, Pentland AP, editors. Graphical models for driver behavior recognition in a smartcar. Intelligent Vehicles Symposium, 2000 IV 2000 Proceedings of the IEEE; 2000: IEEE.
9. Choi Y-G, Lim K-I, Kim J-H, editors. Lane change and path planning of autonomous vehicles using GIS. Ubiquitous Robots and Ambient Intelligence (URAI), 2015 12th International Conference on; 2015: IEEE.
10. Li X, Sun Z, Liu D, Zhu Q, Huang Z, editors. Combining local trajectory planning and tracking control for autonomous ground vehicles navigating along a reference path. Intelligent Transportation Systems (ITSC), 2014 IEEE 17th International Conference on; 2014: IEEE.
11. Chu K, Kim J, Jo K, Sunwoo M. Real-time path planning of autonomous vehicles for unstructured road navigation. International Journal of Automotive Technology. 2015;16(4):653-68.
12. To TB, Meinecke M-M, Schroven F, Nedevschi S, Knaup JC. CityACC—On the way towards an intelligent autonomous driving. Proc 17th World Congr Int Fed Autom Control. 2008:6-11.
13. Sattel T, Brandt T. From robotics to automotive: Lane-keeping and collision avoidance based on elastic bands. Vehicle System Dynamics. 2008;46(7):597-619.
14. Li X, Sun Z, He Z, Zhu Q, Liu D, editors. A practical trajectory planning framework for autonomous ground vehicles driving in urban environments. 2015 IEEE Intelligent Vehicles Symposium (IV); 2015: IEEE.
15. Lan X, Di Cairano S, editors. Continuous curvature path planning for semi-autonomous vehicle maneuvers using RRT. Control Conference (ECC), 2015 European; 2015: IEEE.
16. Wang J, Zhang Q, Zhang Z, Yan X. Structured trajectory planning of collision-free lane change using the vehicle-driver integration data. Science China Technological Sciences. 2016;59(5):825-31.
17. Wang L, Zhao X, Su H, Tang G. Lane changing trajectory planning and tracking control for intelligent vehicle on curved road. SpringerPlus. 2016;5(1):1150.

18. Perumal DG, Subathra B, Saravanakumar G, Srinivasan S. Extended Kalman Filter Based Path-Planning Algorithm for Autonomous Vehicles with I2V Communication. IFAC-PapersOnLine. 2016;49(1):652-7.
19. Zips P, Böck M, Kugi A. Optimisation based path planning for car parking in narrow environments. Robotics and Autonomous Systems. 2016;79:1-11.
20. Sun H, Deng W, Zhang S, Wang S, Zhang Y, editors. Trajectory planning for vehicle autonomous driving with uncertainties. Informative and Cybernetics for Computational Social Systems (ICCSS), 2014 International Conference on; 2014: IEEE.
21. Karaboga D, Akay B. A comparative study of artificial bee colony algorithm. Applied mathematics and computation. 2009;214(1):108-32.
22. ISO I. Mechanical Vibration and Shock--Evaluation of human exposure to whole-body vibrations (2631-1). 1997. International Standards Organization.
23. Solea R, Nunes U, editors. Trajectory planning with velocity planner for fully-automated passenger vehicles. Intelligent Transportation Systems Conference, 2006 ITSC'06 IEEE; 2006: IEEE.
24. Norouzi, A., Masoumi, M., Barari, A., & Sani, S. F. (2018). Lateral control of an autonomous vehicle using integrated backstepping and sliding mode controller. Proceedings of the Institution of Mechanical Engineers, Part K: Journal of Multi-Body Dynamics.

Figure 1. Components of vehicle controlling system in emergency situations.

Figure 2. Path generation assuming the constant velocity for vehicles A and B

Figure 3. Different traffic conditions. (a) Front car has been slowed down, (b) The car behind has been accelerated, (c) Maneuver is not possible due to the unsafe distance

Figure 4. The proposed algorithm

Figure 5. The pseudo-code of Artificial Bee Colony optimization algorithm

Figure 6. Lane changing path and corresponding acceleration using Quintic function

Figure 7. Lane changing paths using Sin function

Figure 8. Lane changing paths based on Septic function

Figure 9. (a) Lane change path using Tangent function; (b) The accelerations of Tangent paths

Figure 10. (a) Various path functions for changing the lane; (b) Accelerations associated with various path functions for changing the lane

Figure 11. Lateral RMS, peak acceleration, and K_a factor values for selected paths

Figure 12. (a) Re-planned paths for changing the lane (case 1); (b) Final path for changing the lane and its corresponding lateral acceleration

Figure 13. Simulation results for case 1 (a) the reference and vehicle paths (b) steering angle (c) lateral acceleration with respect to time (d) yaw rate of vehicle with respect to time

Figure 14. (a) Re-planned paths for changing the lane (case 2); (b) Final path for changing the lane and its corresponding lateral acceleration (case 2)

Figure 15. Simulation results for example 2 (a) the reference and vehicle paths (b) steering angle (c) lateral acceleration with respect to time (d) yaw rate of vehicle with respect to time

Figure 16. (a) Re-planned paths for changing the lane (case 3); (b) Final path for changing the lane and its corresponding lateral acceleration (case 3)

Figure 17. Simulation results for case 3 (a) the reference and vehicle paths (b) steering angle (c) lateral acceleration with respect to time (d) yaw rate of vehicle with respect to time

Figure 18. Variations of RMS against values of b for different values of a (a) The case in which lane change maneuver is possible; (b) lane change maneuver is not possible and the vehicle returns back to initial lane

Figure 19. Variations of RMS against values of b for different values of T_1 ($T_1 > T_2$)

Figure 20. Variations of RMS against values of b for different values of T_1 ($T_1 < T_2$)

Figure 1:

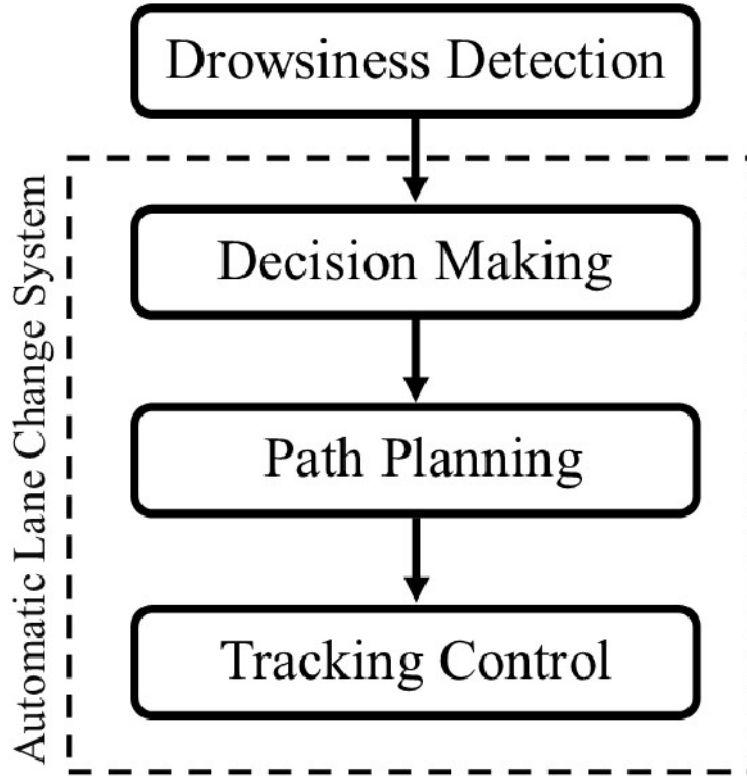


Figure 2:

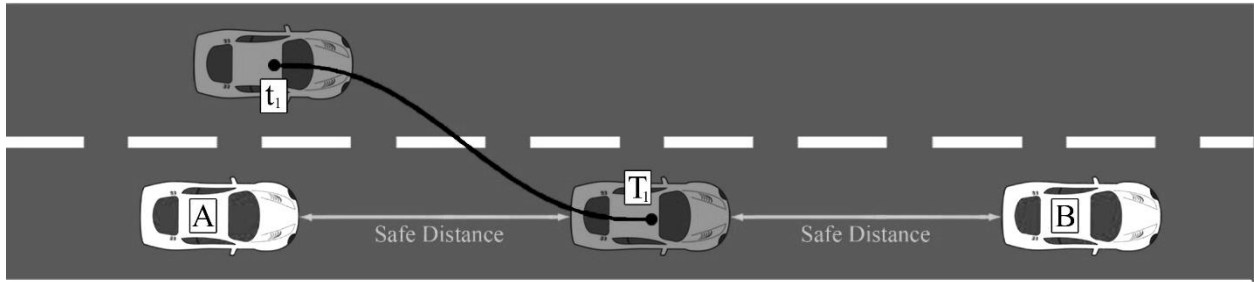
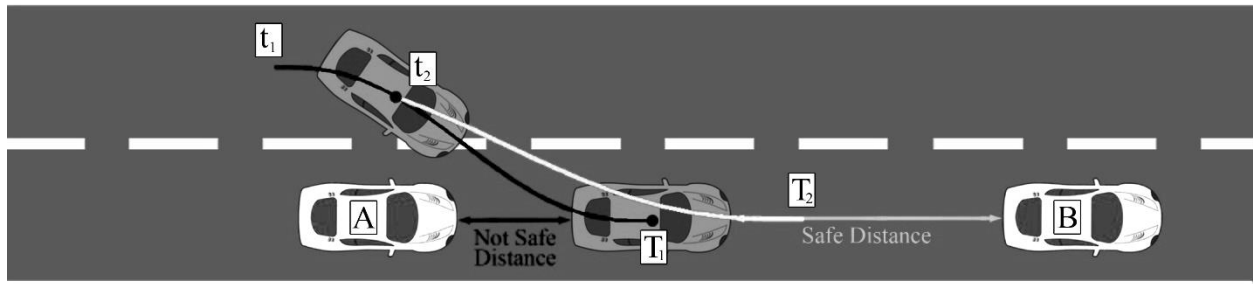
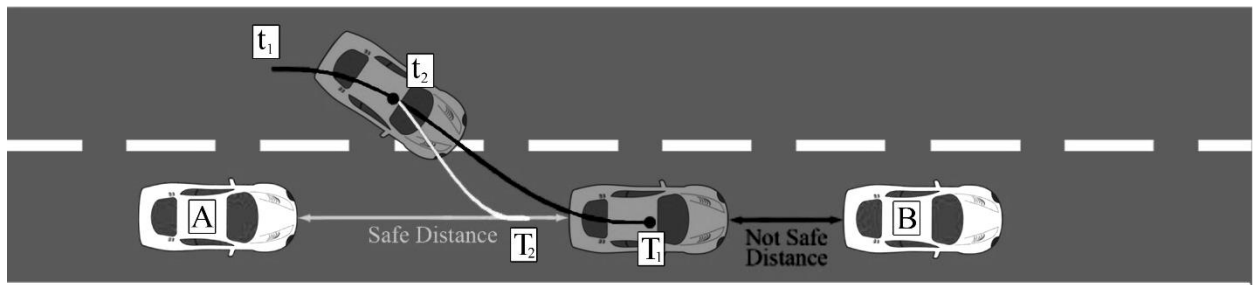


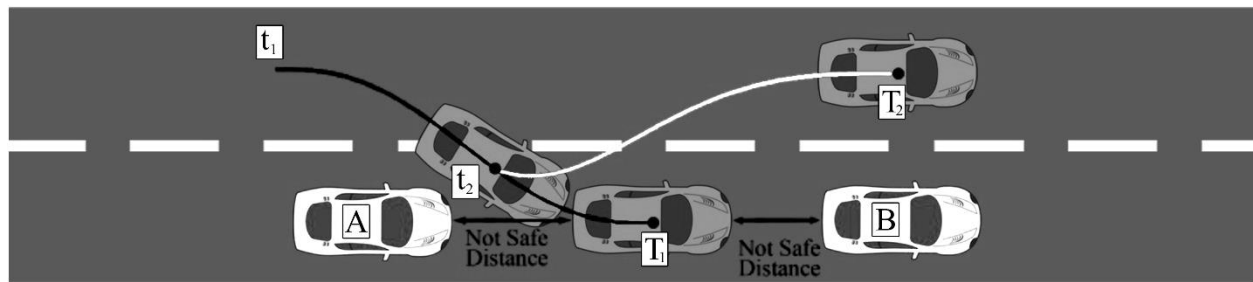
Figure 3:



(a)



(b)



(c)

Figure 4:

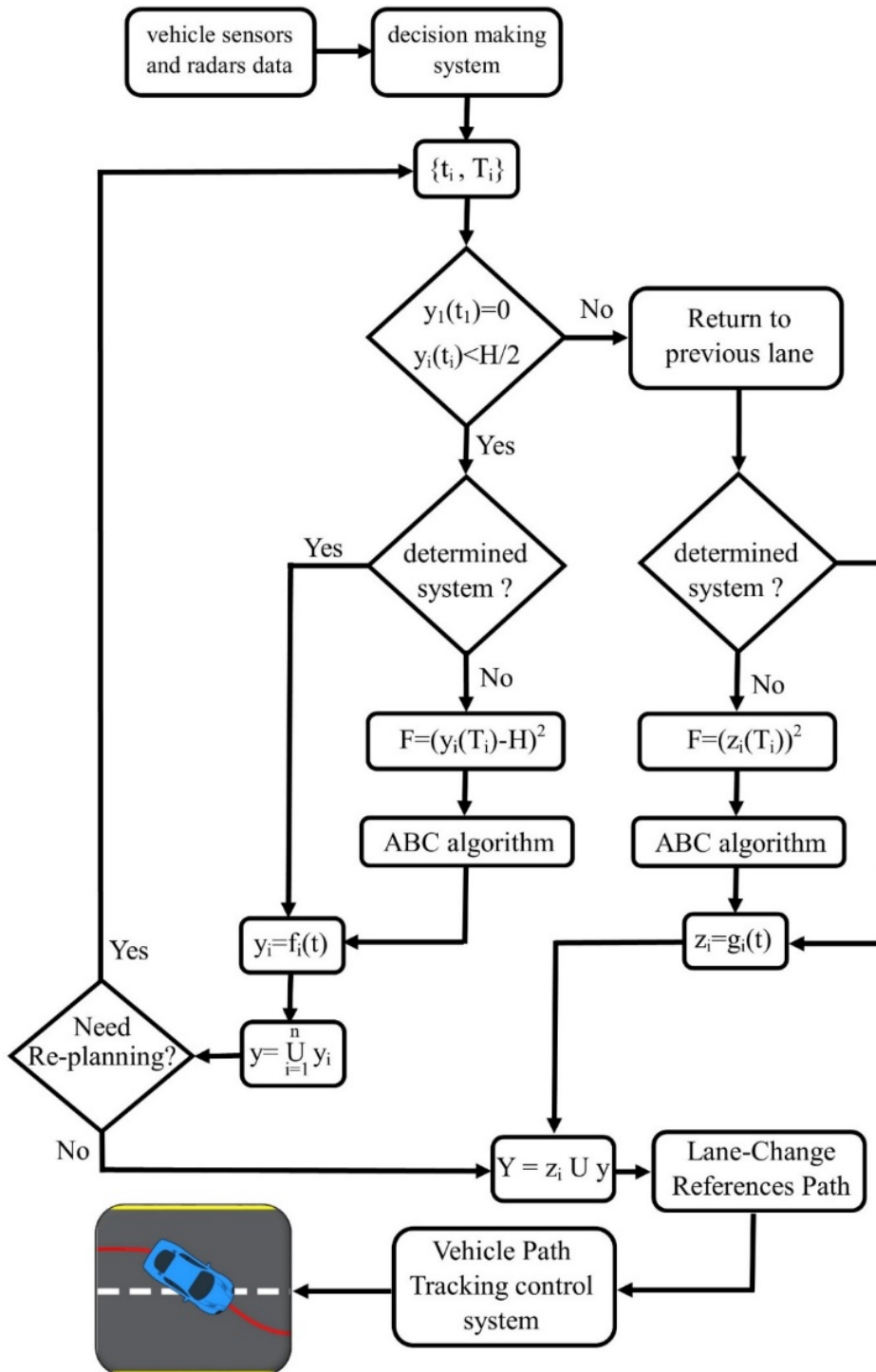


Figure 5:

ABC Algorithm is:

- Set CS to Colony Size
- Set D to Dimension of the Problem
- Set L to $CS * D / 2$
- Initialize parameter sets randomly ($x_{i,j}$)
- Initialize trial to zero for each parameter set
- Compute fitness for each parameter set ($f(x_{i,j})$)
- while termination condition is not satisfied
 - o Set k to a random selected index
 - o Set j to a random selected index
 - o Set ϕ to random number in the range $[-1 \ 1]$
 - o Send employed bees in neighborhood of each parameter set using $v_{i,j} = x_{i,j} + \phi(x_{i,j} - x_{k,j})$
 - o Compute fitness for each employed bees
 - o If fitness of $v_{i,j}$ is better than $x_{i,j}$
 - replace old parameter set with new set
 - $trial_{i,j} = 0$
 - o else
 - increment $trial_{i,j}$
 - o Calculate the probability values for all sets based on their fitness
 - o Set i to an index selected based on probabilities
 - o Set k to a random selected index
 - o Set j to a random selected index
 - o Set ϕ to random number in the range $[-1 \ 1]$
 - o Send onlooker bees in neighborhood of parameter sets using $v_{i,j} = x_{i,j} + \phi(x_{i,j} - x_{k,j})$
 - o Compute fitness for each onlooker bees
 - o If fitness of $v_{i,j}$ is better than $x_{i,j}$
 - replace old parameter set with new set
 - $trial_{i,j} = 0$
 - o Otherwise,
 - increment $trial_{i,j}$
 - o Memorize best parameter set
 - o If $trial_{i,j}$ is greater than L
 - Generate a new parameter set randomly and replace it

Figure 6:

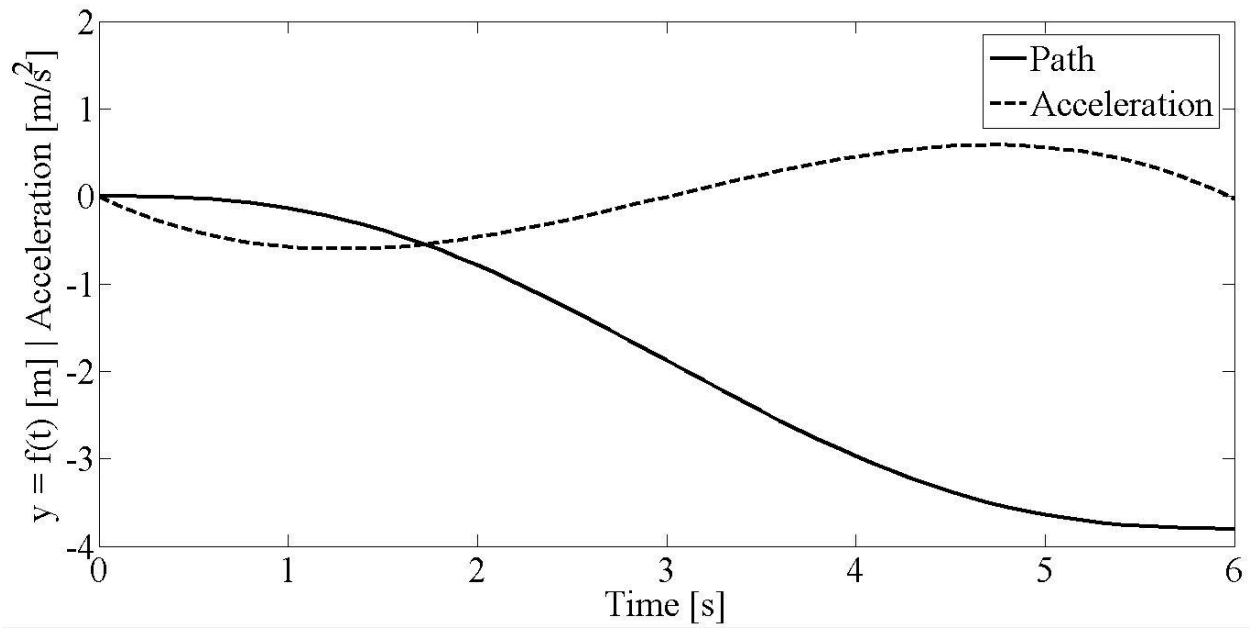


Figure 7:

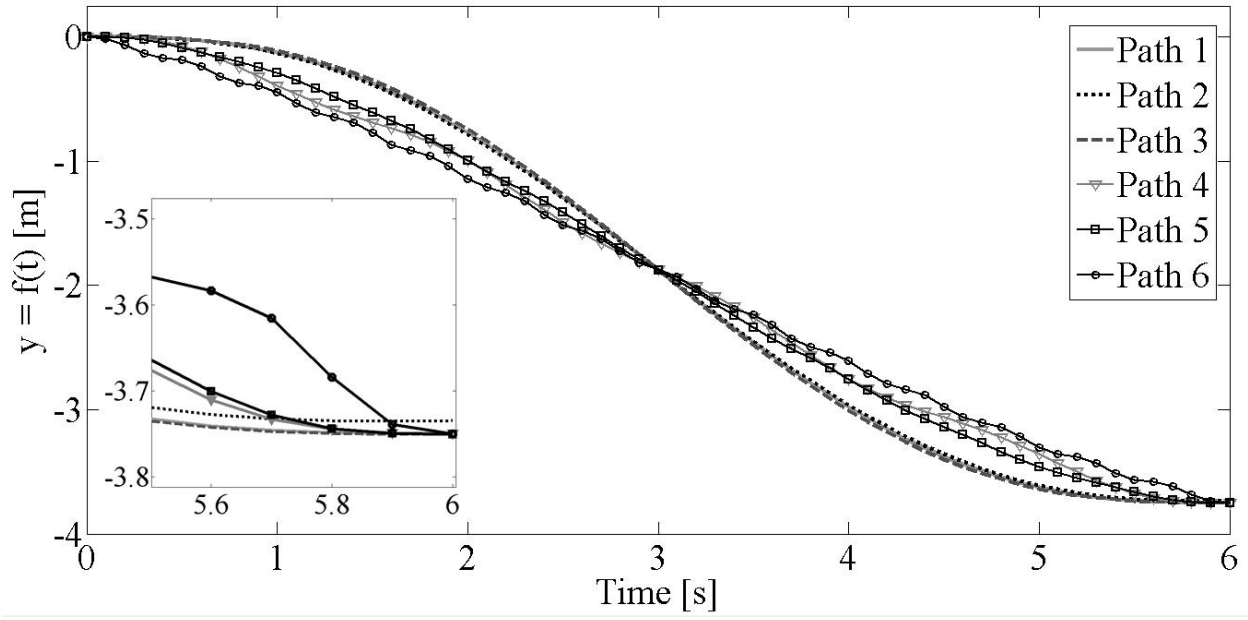


Figure 8:

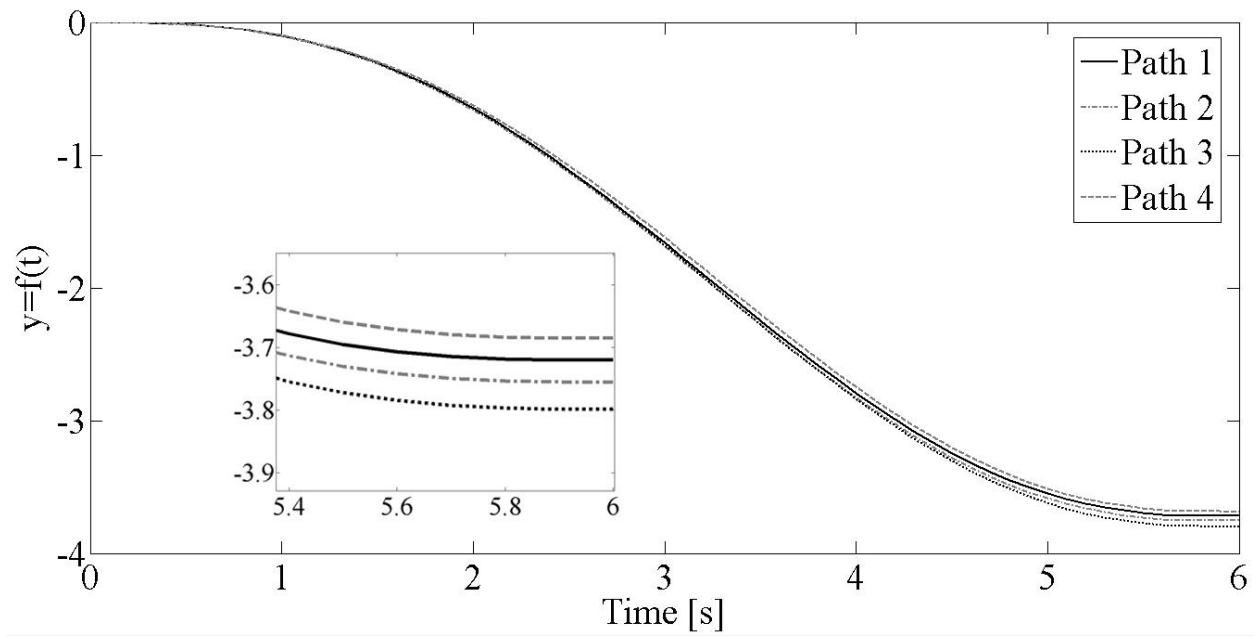


Figure 9:

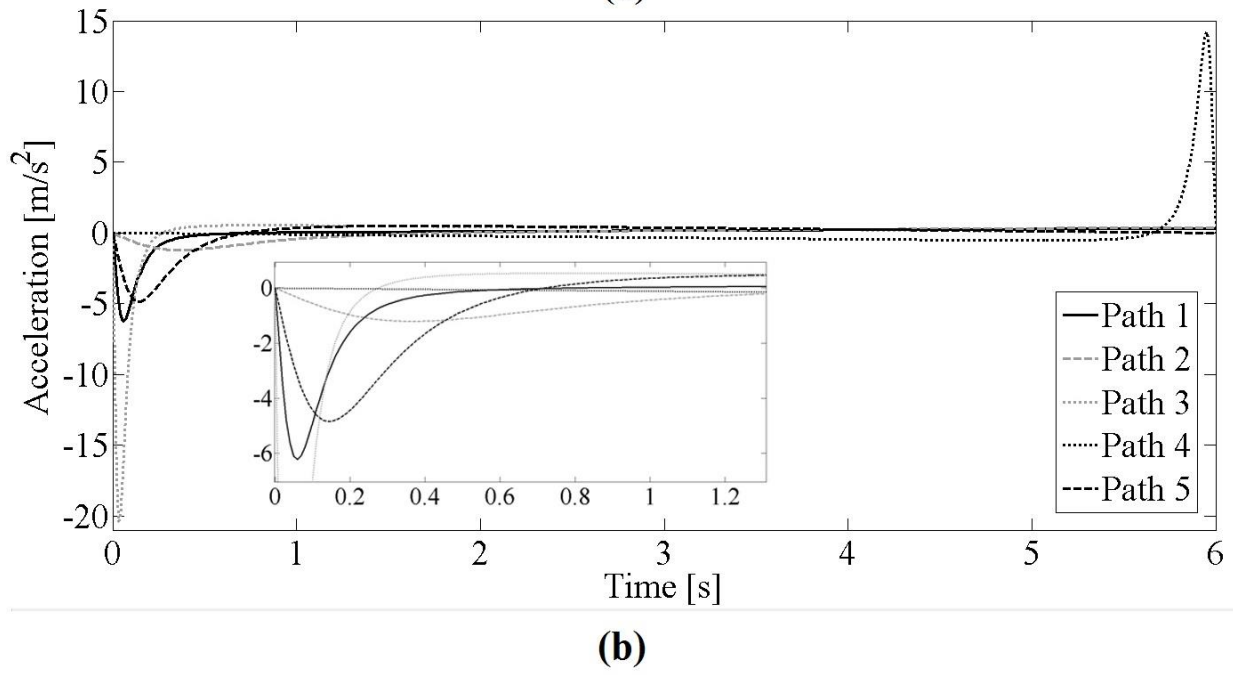
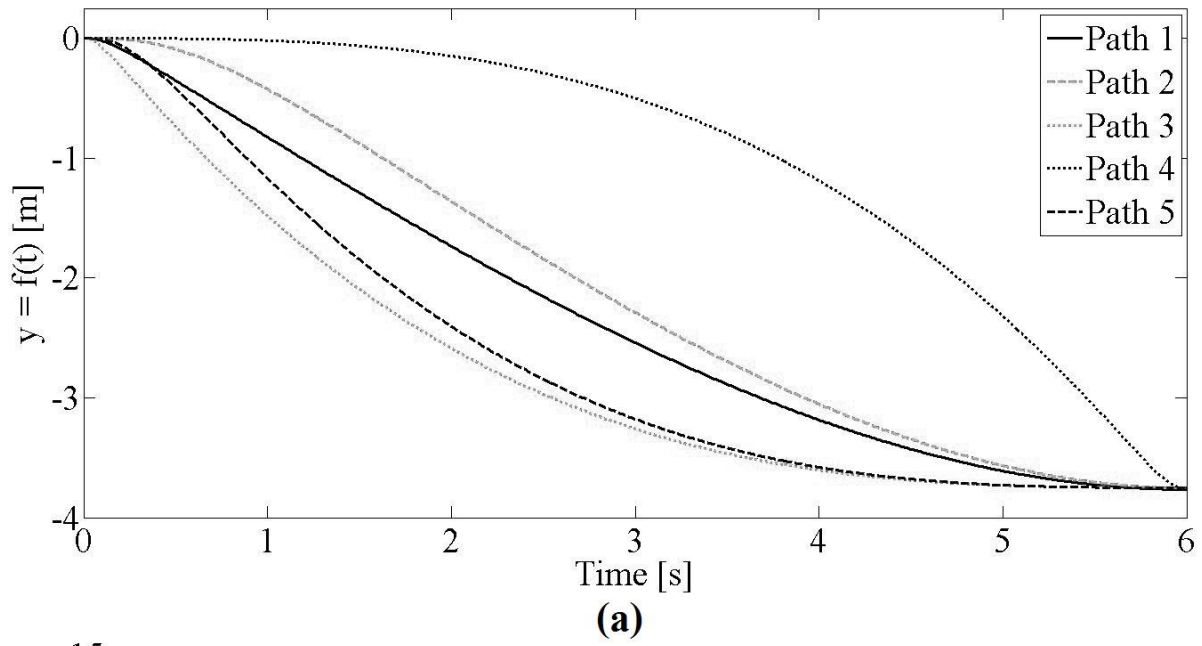
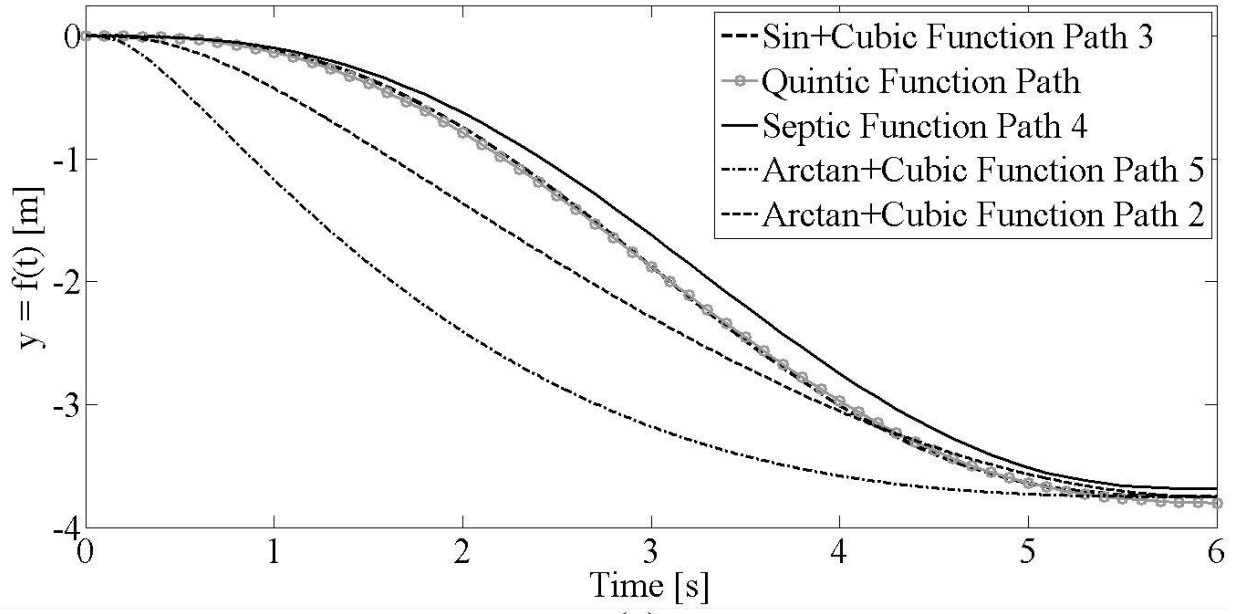
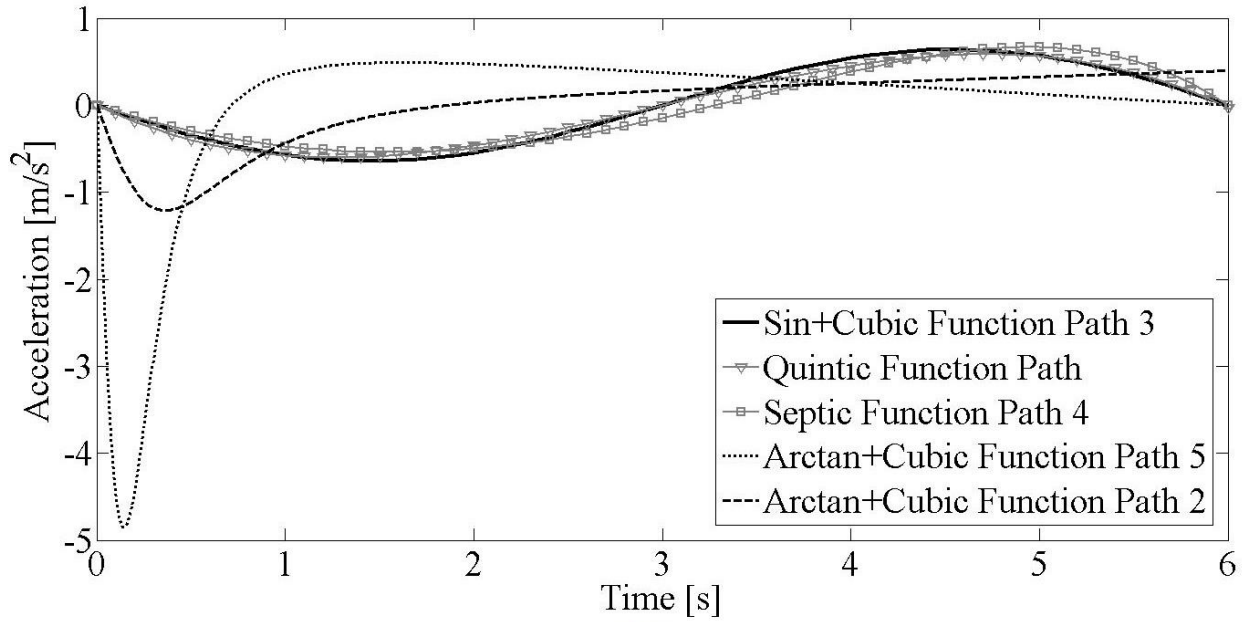


Figure 10:



(a)



(b)

Figure 11:

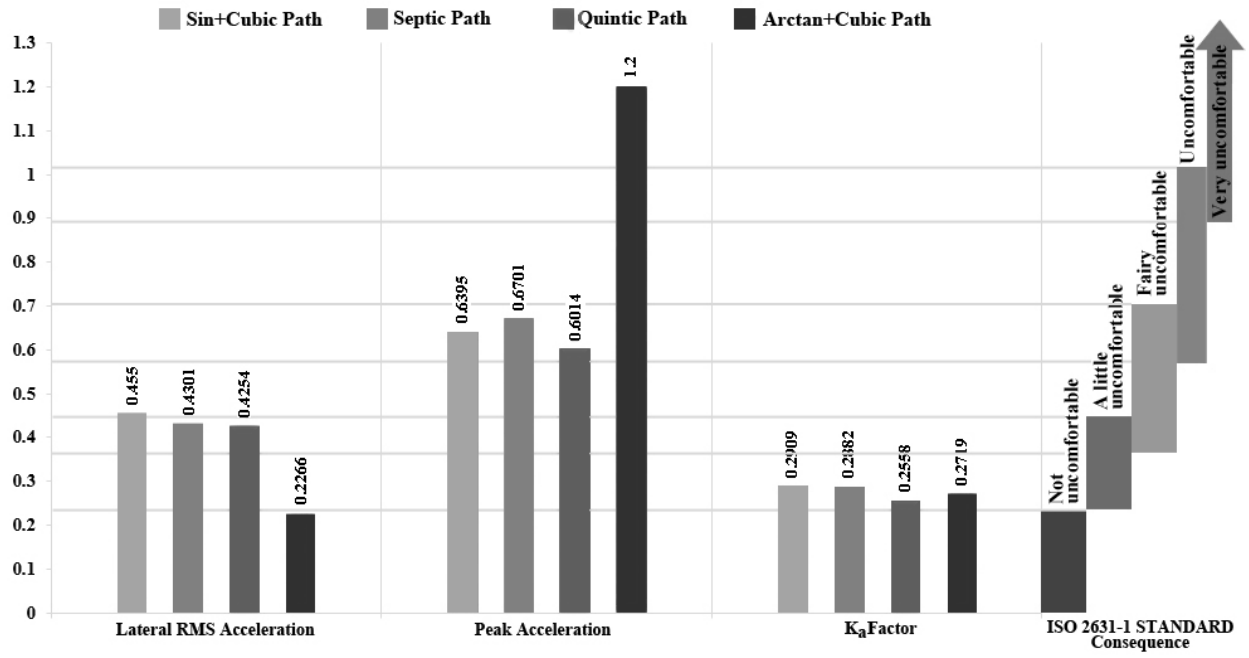
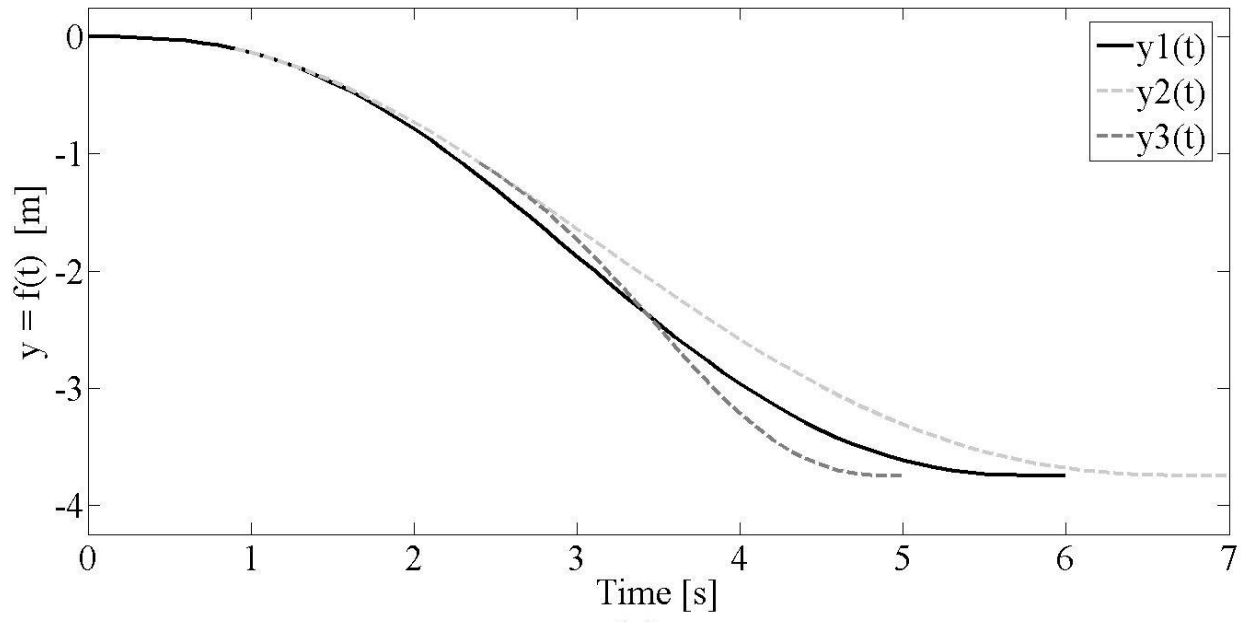
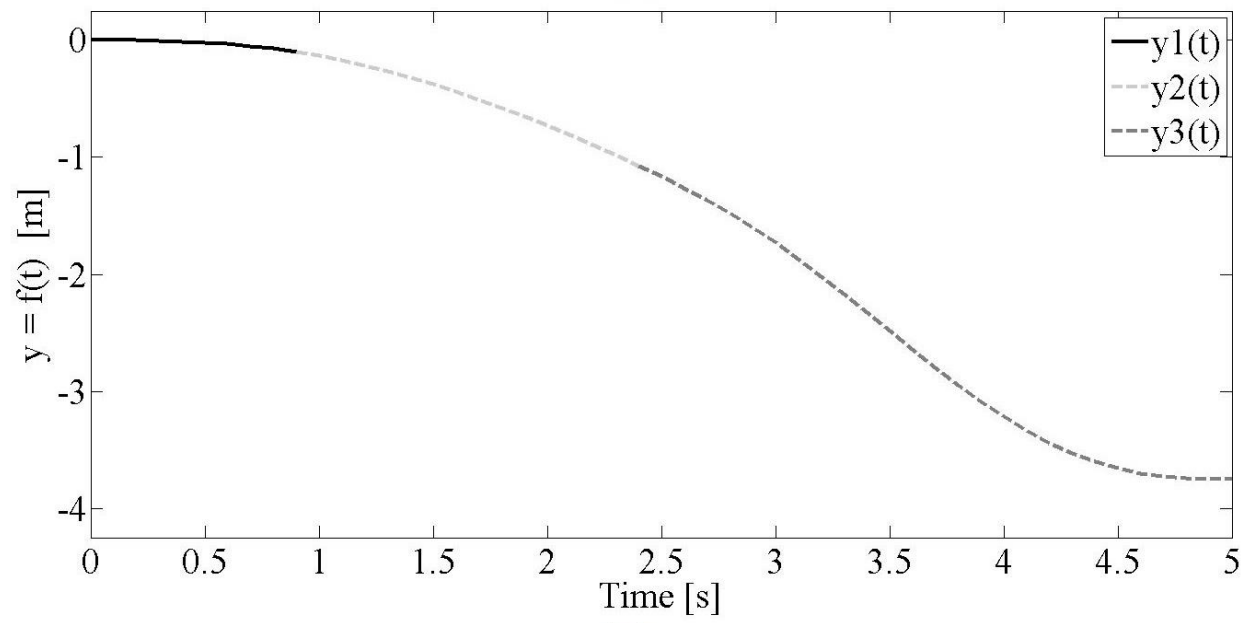


Figure 12:



(a)



(b)

Figure 13:

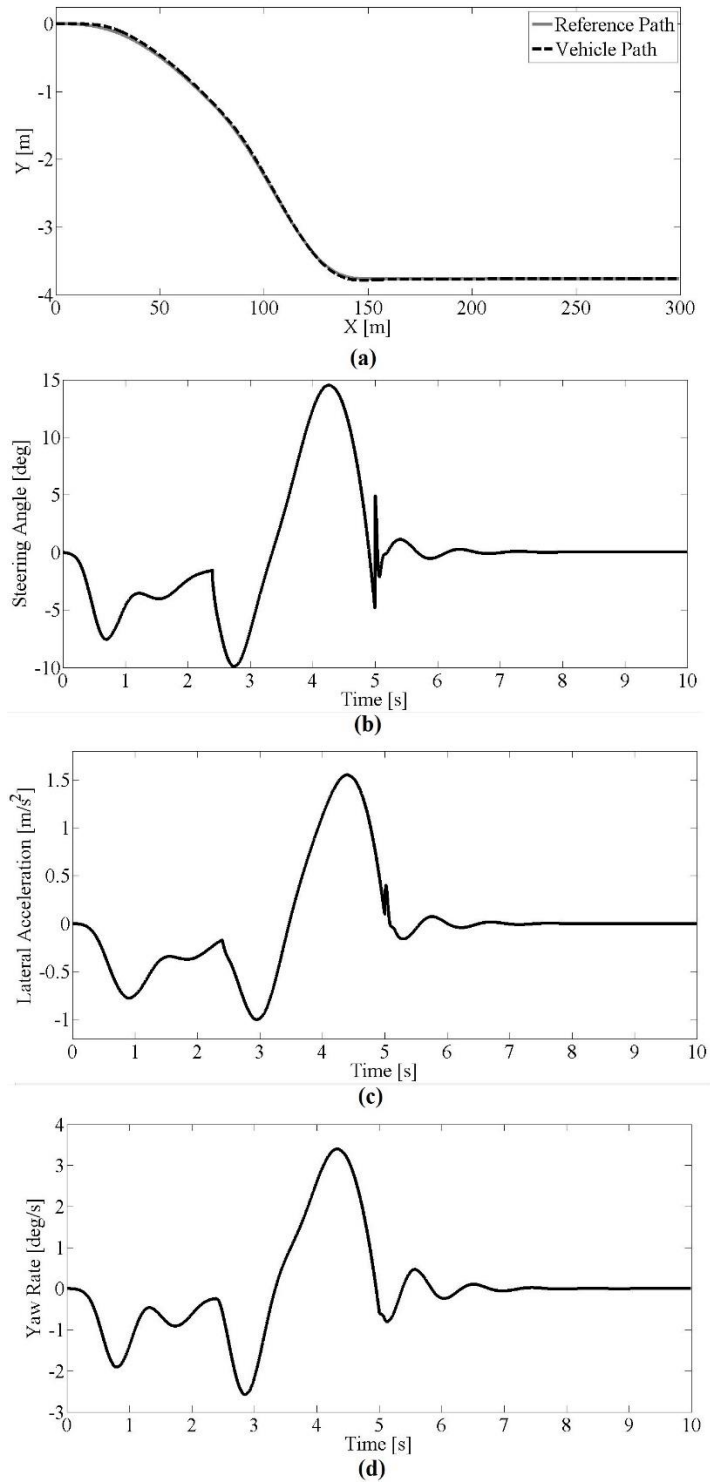


Figure 14:

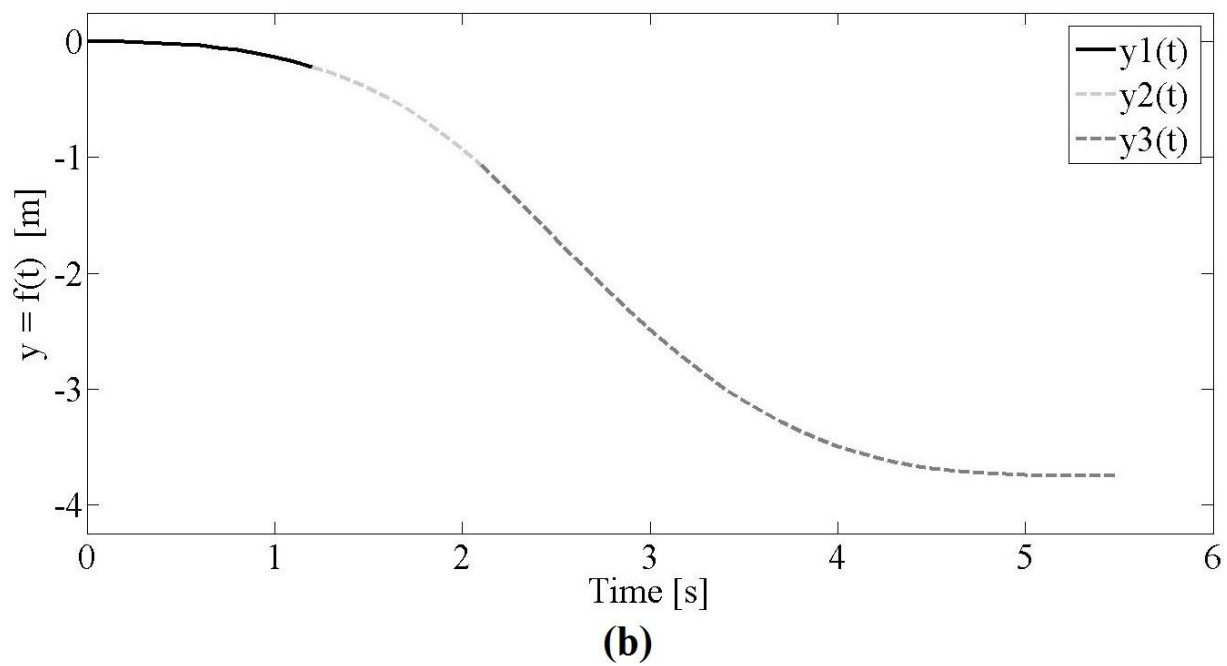
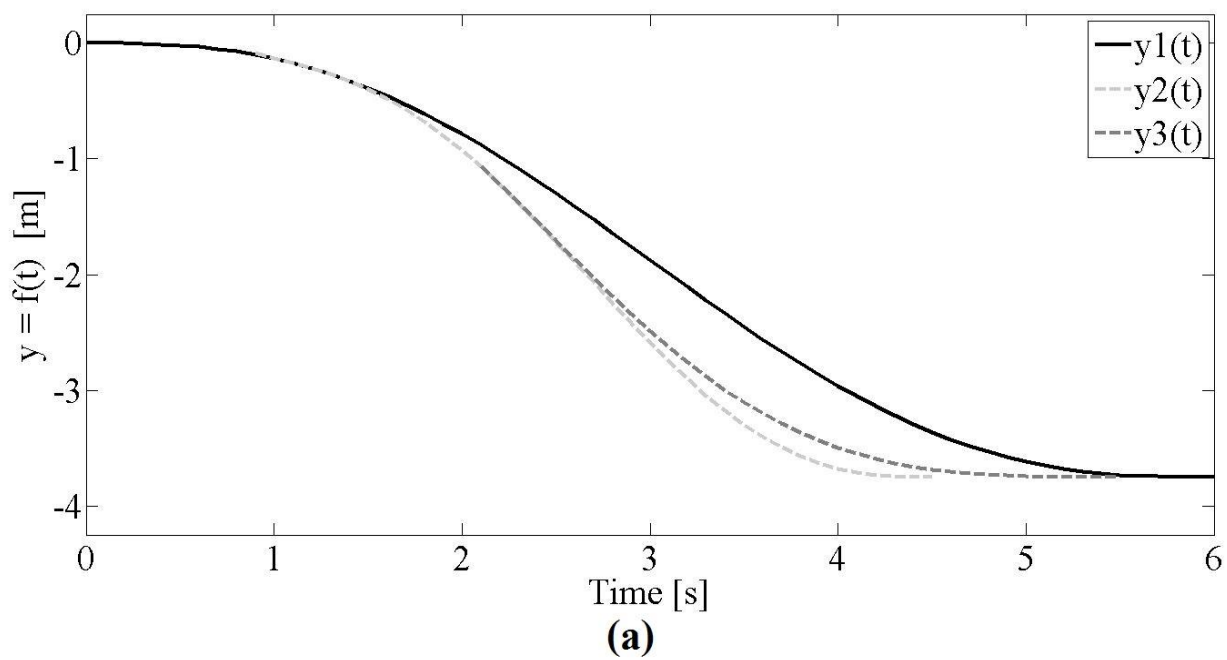


Figure 15:

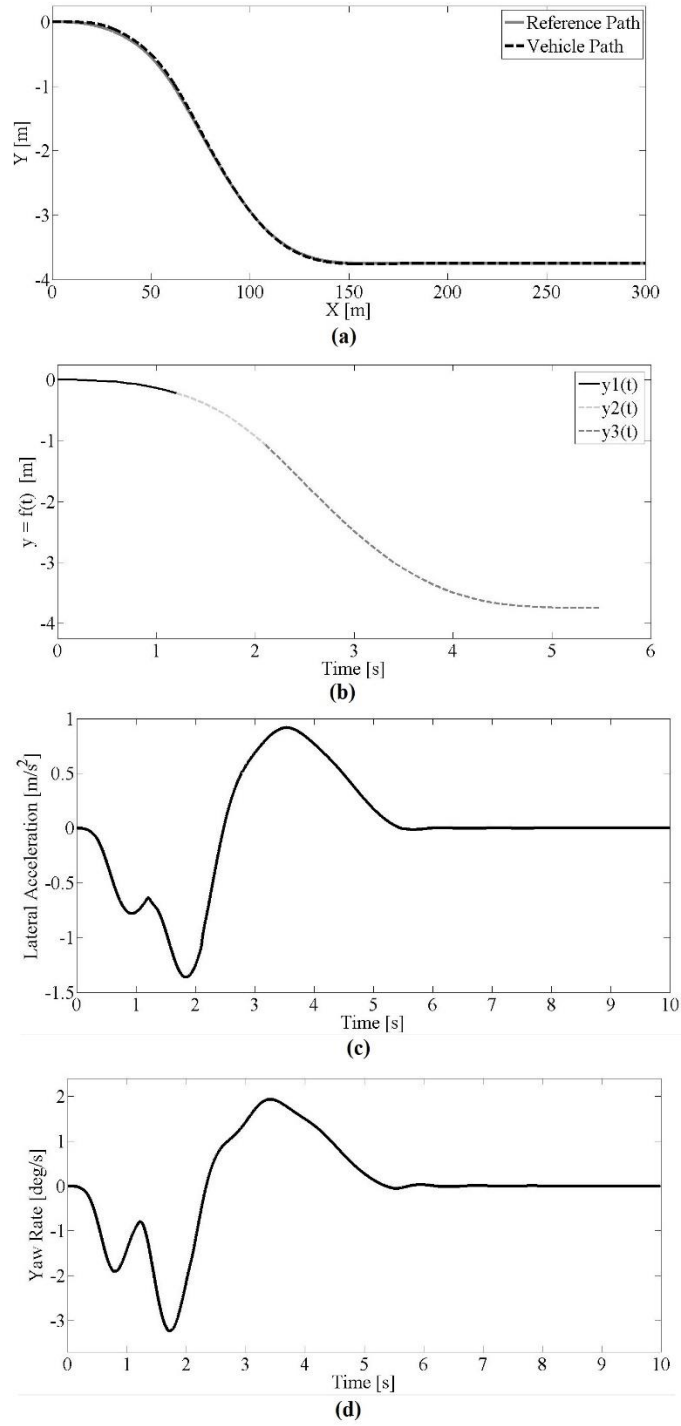


Figure 16:

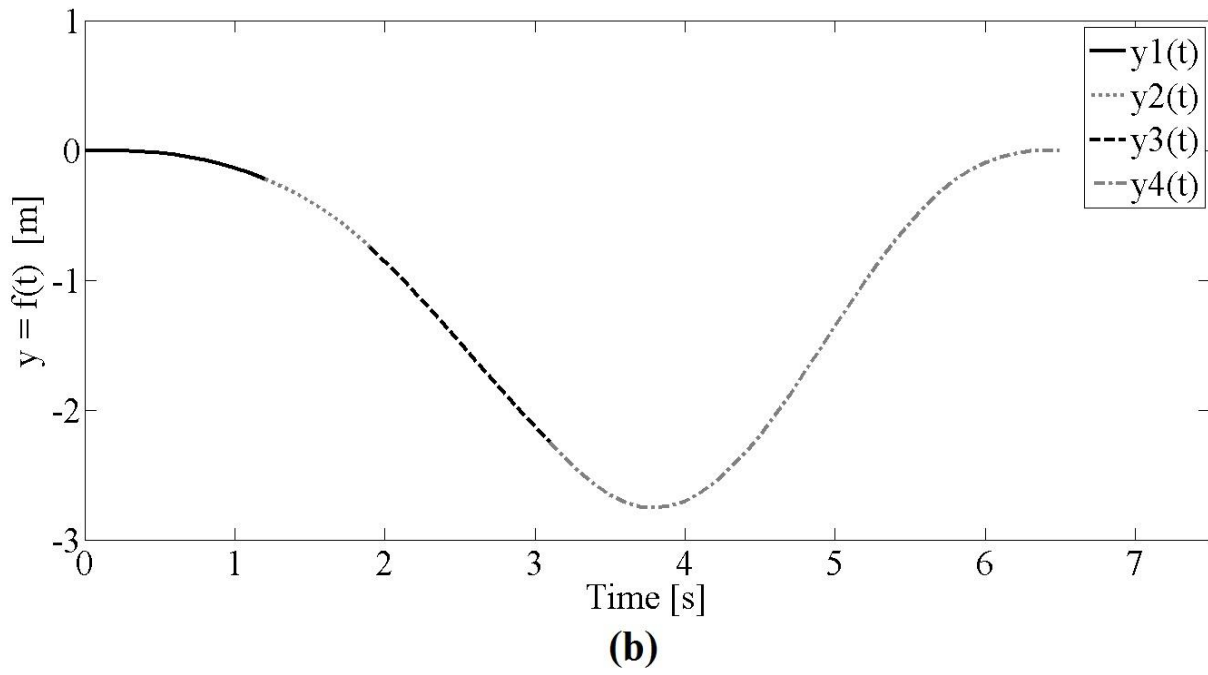
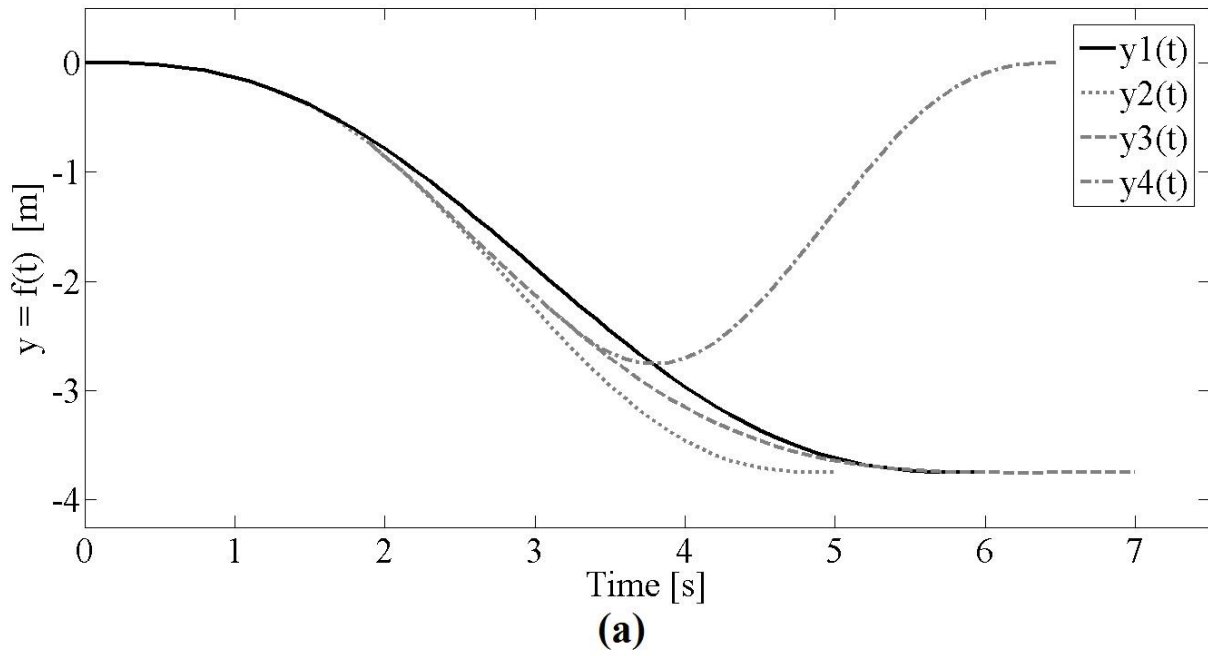
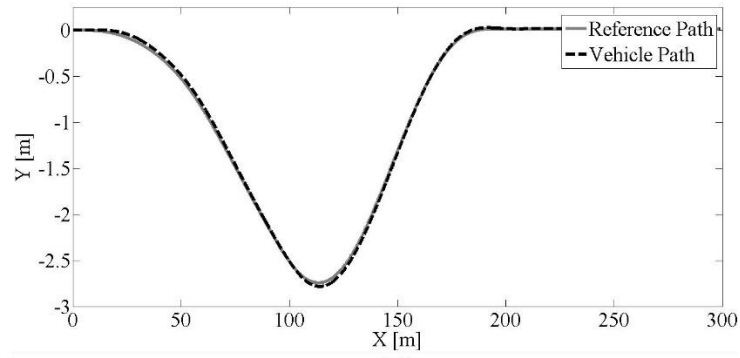
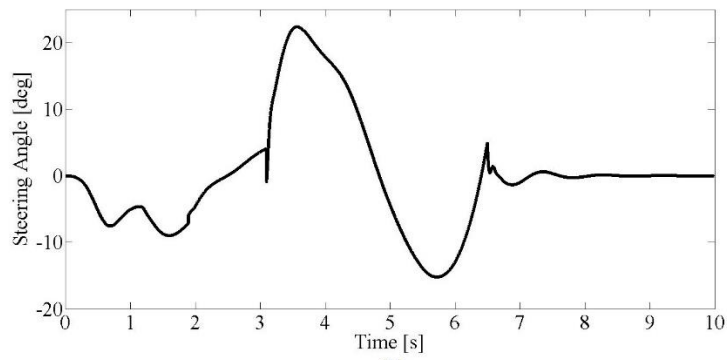


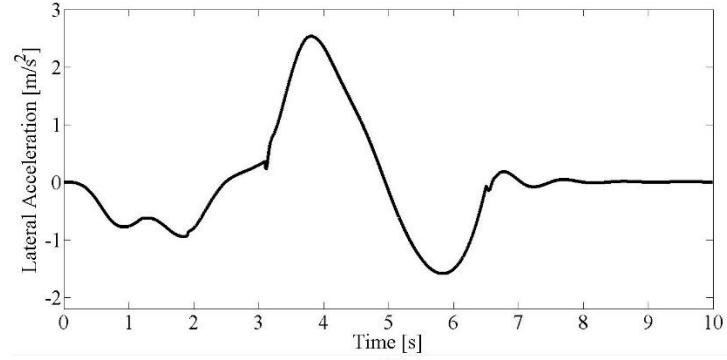
Figure 17:



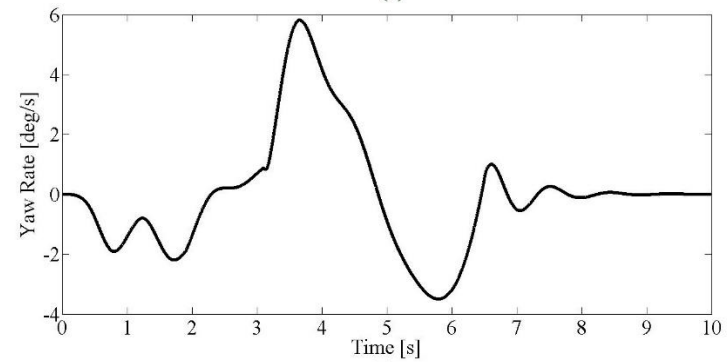
(a)



(b)



(c)



(d)

Figure 18:

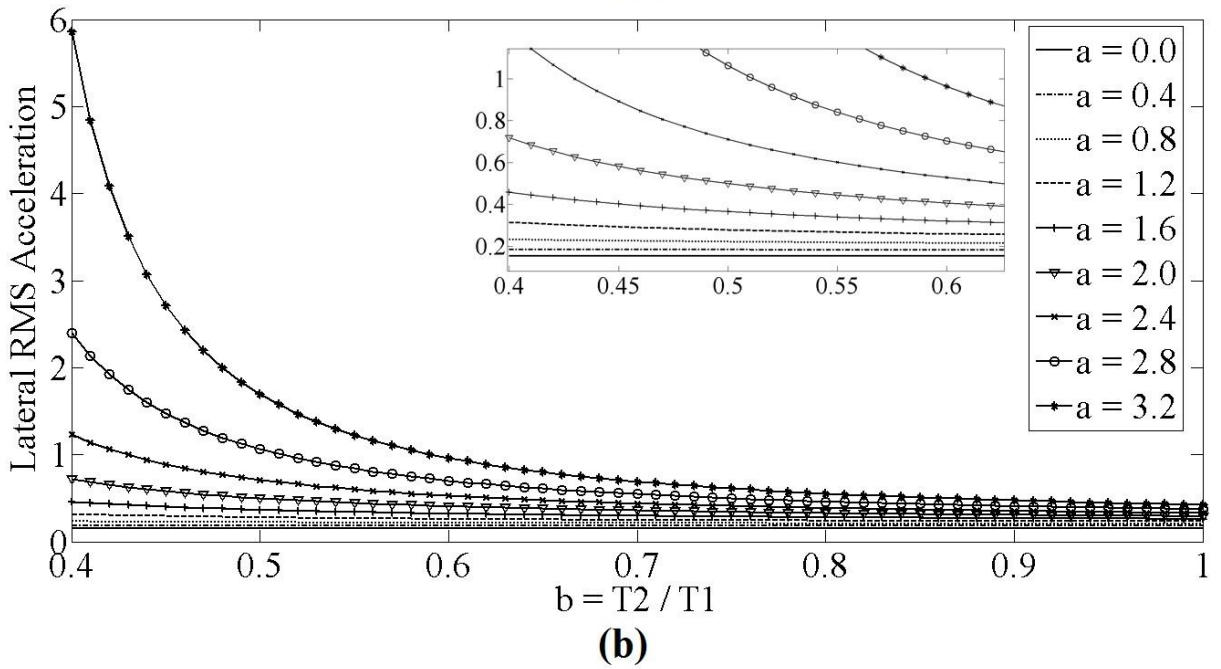
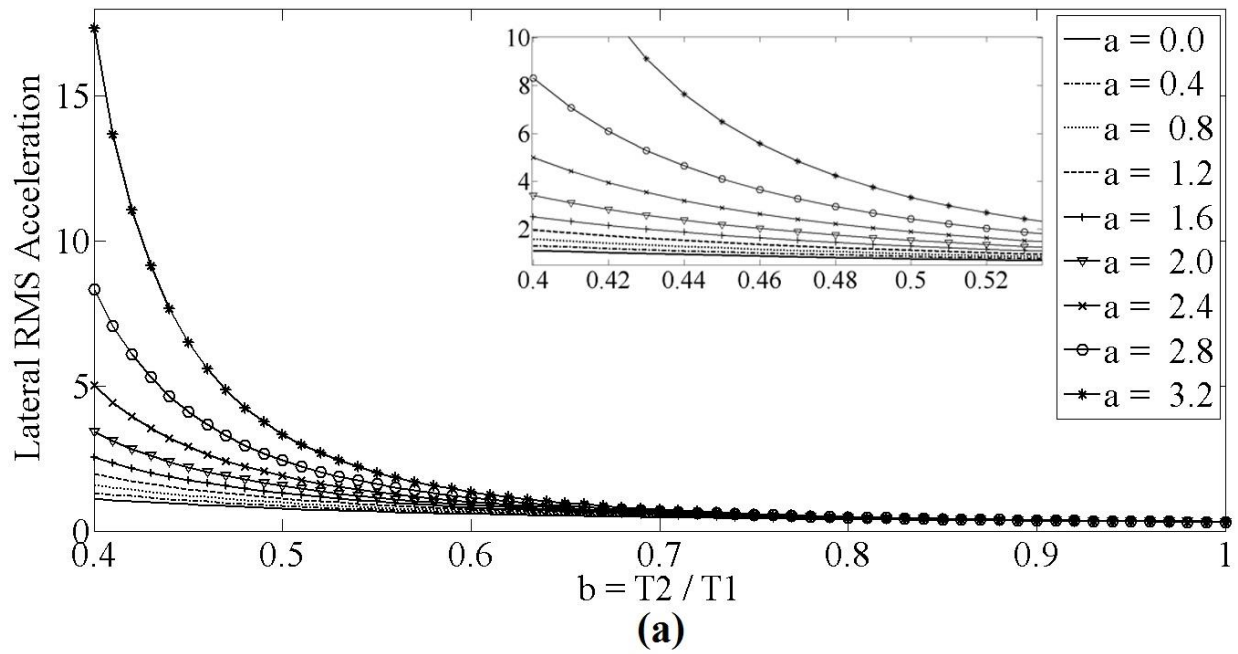


Figure 19:

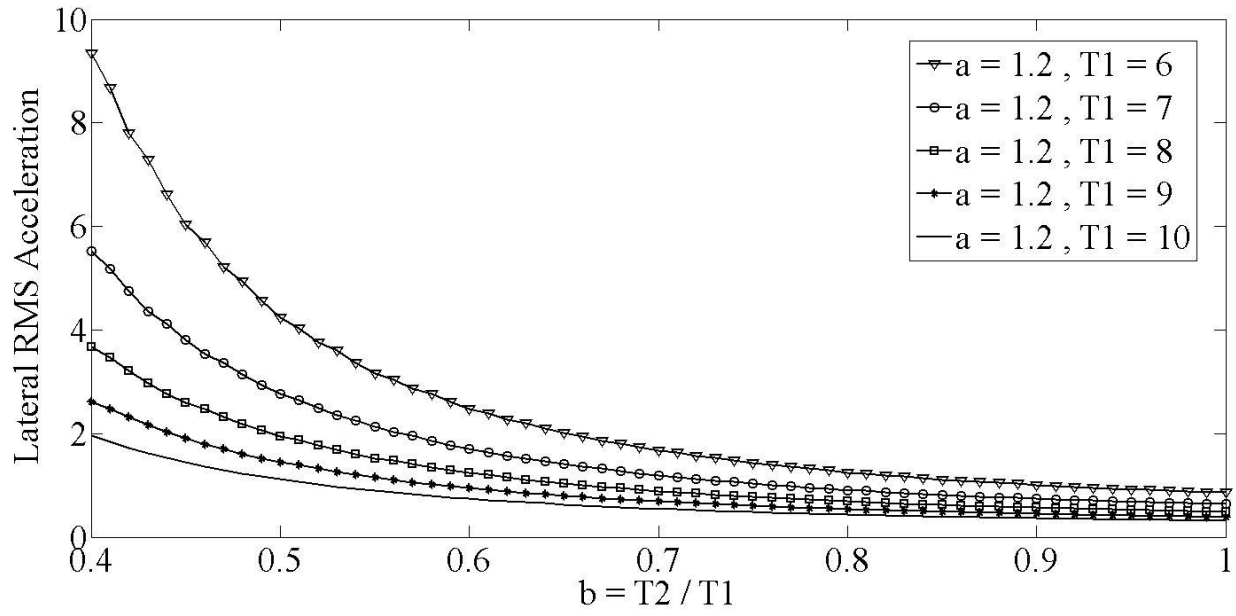


Figure 20:

